Brillouin scattering from shear horizontal surface phonons in buried SiO_2 layers

1994 J. Phys.: Condens. Matter 6 L85

(http://iopscience.iop.org/0953-8984/6/6/010)

J. Phys.: Condens. Matter 6 (1994) L85–L91. Printed in the UK

LETTER TO THE EDITOR

Brillouin scattering from shear horizontal surface phonons in buried SiO_2 layers

C E Bottani, G Ghislotti and P Mutti

Dipartimento di Ingegneria Nucleare del Politecnico di Milano, Via Ponzio, 34/3 - 20133 Milano, Italy

Received 11 October 1993, in final form 15 November 1993

Abstract. Experimental evidence and a theoretical explanation of Brillouin scattering from shear horizontal surface acoustic phonons in an Si buffer with a buried SiO_2 layer are given in both the discrete and continuum parts of the spectrum. This is the first experimental observation of Brillouin scattering from shear horizontal acoustic phonons in the continuum spectral region. The intensity and position of peaks in Brillouin spectra have been qualitatively described in terms of the layer projected phonon density of states calculated for such a structure.

Brillouin scattering from solid surfaces has been shown to be an excellent technique to study the spectrum of long-wavelength surface acoustic excitations of thermal origin in opaque materials. Recently the problem of calculating the normal modes of vibration of elastic half spaces [1] and layered media [2] has been theoretically considered in order to evaluate the Brillouin scattering cross section from surface acoustic phonons. Experimentally, using tandem multi-pass interferometry [3], it has been possible to observe surface acoustic phonons in solid substrates [4] and supported films [5–7] but most of the studies have dealt with surface acoustic phonons polarized in the sagittal plane, defined by the surface phonon propagation wavevector, $Q_{\|}$, and the surface normal. For these, light scattering occurs through the ripple and elasto-optic effects and the Brillouin scattering cross section, which depends on a combination of both these mechanisms, can show strong interference features [6]. Calculations of Brillouin scattering cross section from shear horizontal (SH) surface acoustic modes† have been performed in layered media by several authors [2, 8]. The mechanism of interaction is only elasto-optic and no interference effects appear in the spectrum. The only reported experimental work on the detection of SH surface acoustic phonons using Brillouin scattering was conducted by Bell *et al* [9] in an Nb/Cu superlattice on a sapphire substrate. Those authors performed their measurements by detecting the tails of the acoustic modes in the sapphire substrate and gave no evidence of SH acoustic modes in the continuum part of the spectrum.

In the present letter we intend to discuss the observation of SH surface acoustic modes in both the discrete and continuum parts of the spectrum using Brillouin scattering in a structure that consists of an SiO_2 layer buried in an Si(001) substrate. The thickness of the buried oxide and top Si layer was measured by cross-sectional transmission electron microscopy to be respectively 110 and 350 nm. Observations were conducted for phonons propagating along ⟨100⟩ and ⟨110⟩. For these directions the SH motion is decoupled from

† In the discrete part of the spectrum these modes are called Love modes [8].

0953-8984/94/060085+07$07.50

the sagittal one. The spectrum of SH long-wavelength acoustic phonons in a semi-infinite layered medium is, in general, the union of a discrete and a continuum part. The latter starts at the transverse threshold of the substrate $\omega_t = c_t Q_{\|}$, where c_t is the shear horizontal sound velocity of the substrate. Strictly speaking only the discrete eigenvalues correspond to true surface modes (*bounded states or resonances*). Yet also in the continuum spectrum one can find considerable structure of surface character (*quasi-resonances or pseudo-surface modes*). The degree of surface character of these collective excitations can be judged from inspection of the layer projected phonon density of states (LPPDS, see below). Since the system is translationally invariant in the wave propagation direction x, $Q_{\|}$ is a 'good quantum number' and the $(\omega, Q_{\|})$ Fourier component of the u_y SH displacement field can be written as

$$u_y(\omega, Q_{\|}; x, z, t) = \exp[i(Q_{\|}x - \omega t)]\phi(\omega, Q_{\|}, z). \tag{1}$$

For propagation along $\langle 100 \rangle$ the mode z-profiles $\phi(\omega, Q_{\|}, z)$ are the real eigenfunctions of the self-adjoint Liouville equation [10]

$$\frac{\mathrm{d}}{\mathrm{d}z}\left[C_{44}(z)\frac{\mathrm{d}\phi(\omega, Q_{\|}, z)}{\mathrm{d}z}\right] + [\rho(z)\omega^2(Q_{\|}) - C_{44}(z)Q_{\|}^2]\phi(\omega, Q_{\|}, z) = 0 \tag{2}$$

corresponding to the real eigenvalues $\omega^2(Q_{\|})$. The functions $\rho(z)$ and $C_{44}(z)$ take within each layer the constant value of the mass density and C_{44} elastic constant of the corresponding material. A similar Liouville equation is obtained for the $\langle 110 \rangle$ case substituting $\frac{1}{2}[C_{11}(z) - C_{12}(z)]$ for $C_{44}(z)$ as the multiplying coefficient of $Q_{\|}^2$. Together with appropriate boundary conditions and the normalization condition (we adopted a *slab approximation*)

$$\int_{\text{slab thickness}} \rho(z)\phi^2(\omega, Q_{\|}, z)\,\mathrm{d}z = 1$$

equation (2) constitutes a singular (at least in the case of sharp interfaces) Sturm–Liouville eigenvalue problem [10]. We solved the problem numerically using free surface boundary conditions. Literature values for density and elastic constants of Si [11] and fused SiO_2 [12] were taken.

From the spectral expansion of the retarded and advanced Green functions of (2) computed at $z = z'$

$$\langle\langle u_y(z); u_y(z)\rangle\rangle_{\omega \mp i\epsilon, Q_{\|}} = \sum_{\alpha} \frac{\phi_\alpha^2(Q_{\|}, z)}{(\omega \mp i\epsilon)^2 - \omega_\alpha^2(Q_{\|})} \tag{3}$$

a smooth representation $\bar{g}_{yy}(\omega, Q_{\|}|z, z)$ of the LPPDS for SH phonons

$$g_{yy}(\omega, Q_{\|}|z, z) = \sum_{\alpha} \rho(z)\phi_\alpha^2(Q_{\|}, z)\delta[(\omega - \omega_\alpha(Q_{\|})] \tag{4}$$

can be obtained as

$$\bar{g}_{yy}(\omega, Q_{\|}|z, z) = \frac{\rho(z)}{2\pi i}[\langle\langle u_y(z); u_y(z)\rangle\rangle_{\omega - i\epsilon, Q_{\|}} - \langle\langle u_y(z); u_y(z)\rangle\rangle_{\omega + i\epsilon, Q_{\|}}]. \tag{5}$$

Brillouin spectra were acquired in backscattering at room temperature using a 3 + 3 passes tandem interferometer [3]. Measurements were performed using incident p-polarized

light from an Ar ion laser oscillating in single longitudinal mode at $\lambda_0 = 514.5$ nm wavelength. The laser power onto the sample surface was 150 mW. Spectra were taken at different angles of incidence, from 20° to 70°, in order to have different wavevector components parallel to the surface $Q_{||}$. In backscattering this is given by $Q_{||} = 2k_0 \sin\theta$ where θ is the angle of incidence and $k_0 = 2\pi/\lambda_0$ is the modulus of the incident photon wavevector. To compensate for the parasitic broadening caused by the finite collection aperture, a vertical slit ($\Delta\theta \simeq \pm 2°$) was used in the collection. This had also the advantage of avoiding the splitting of Brillouin scattering peaks in the spectra caused by the interception of the backscattered photons by the mirror used to direct the incident light onto the sample. With this configuration the integration time ranged from 2 to 4 h per measurement.

The Brillouin spectrum taken along ⟨100⟩ at $\theta = 60°$ is presented as the lower trace of figure 1(*a*). In this measurement no analysis of the polarization of the scattered light was conducted. Two peaks, labelled RW and SH2, are clearly visible, that lying at lower frequency presenting a small shoulder labelled as SH1. Peak SH2 and the shoulder SH1 were identified as being due to scattering from SH acoustic modes while peak RW was due to the Rayleigh wave propagating at the free surface.

The shear horizontal character of peaks SH1 and SH2 can be ascertained by the analysis of the p–s spectrum taken under the same experimental conditions and presented as the upper trace of figure 1(*a*). Only the elasto-optic coupling mechanism gives a contribution to the p–s cross section. In our scattering geometry, for ⟨100⟩, the y-component E_y (s polarized) of the scattered electric field is radiated by a fluctuating polarization vector P_y given, for cubic and isotropic materials, by [6]

$$P_y = \tfrac{1}{2}\epsilon_0 k_{44}(z)\left(\frac{\partial u_y}{\partial x}E_x + \frac{\partial u_y}{\partial z}E_z\right) \tag{6}$$

where ϵ_0 is the vacuum dielectric constant. The function $k_{44}(z)$ takes within each layer the value of the k_{44} elasto-optic coefficient of the corresponding material ($k_{44}^{\mathrm{Si}} = 23.4$ [14], $k_{44}^{\mathrm{SiO_2}} = 0.345$ [15]). E_x and E_z are, in the Born approximation, the Cartesian components of the incident electric field in the sagittal plane (p polarized) propagated to the point (x, z). A relation similar to (6) holds for ⟨110⟩. From equation (6) it is evident that only the shear horizontal displacement field u_y (see equation (1)) can contribute to the p–s cross section. Apart from RW no other modes of sagittal character (Sezawa modes) are visible in the depolarized Brillouin spectrum of figure 1(*a*). This might be due to interference effects in the Brillouin cross section for sagittal modes in this geometry [2, 6].

The spectrum taken at $\theta = 30°$, shown in figure 1(*b*), exhibits the same group of peaks displaced in their relative position and with a different ratio of intensity. The intensity of peak SH1 is increased while peak SH2 appears slightly broadened.

We found that a qualitative explanation of the experimental results can be given by considering the following integral of the LPPDS:

$$S_{yy}(\omega, Q_{||}) = \int_0^d \bar{g}_{yy}(\omega, Q_{||}|z, z)\,\mathrm{d}z. \tag{7}$$

$S_{yy}(\omega, Q_{||})$ was evaluated in a region between the free surface and a depth $d = 1000$ nm corresponding approximately to the optical penetration depth in Si [11] evaluated at 514.5 nm. Results corresponding to 60° and 30° incidence are plotted as dashed lines in figures 1(*a*) and (*b*) respectively. The experimental spectra show an increase in the magnitude of peak SH1 relative to SH2 for 30° incidence with respect to 60°. This is in

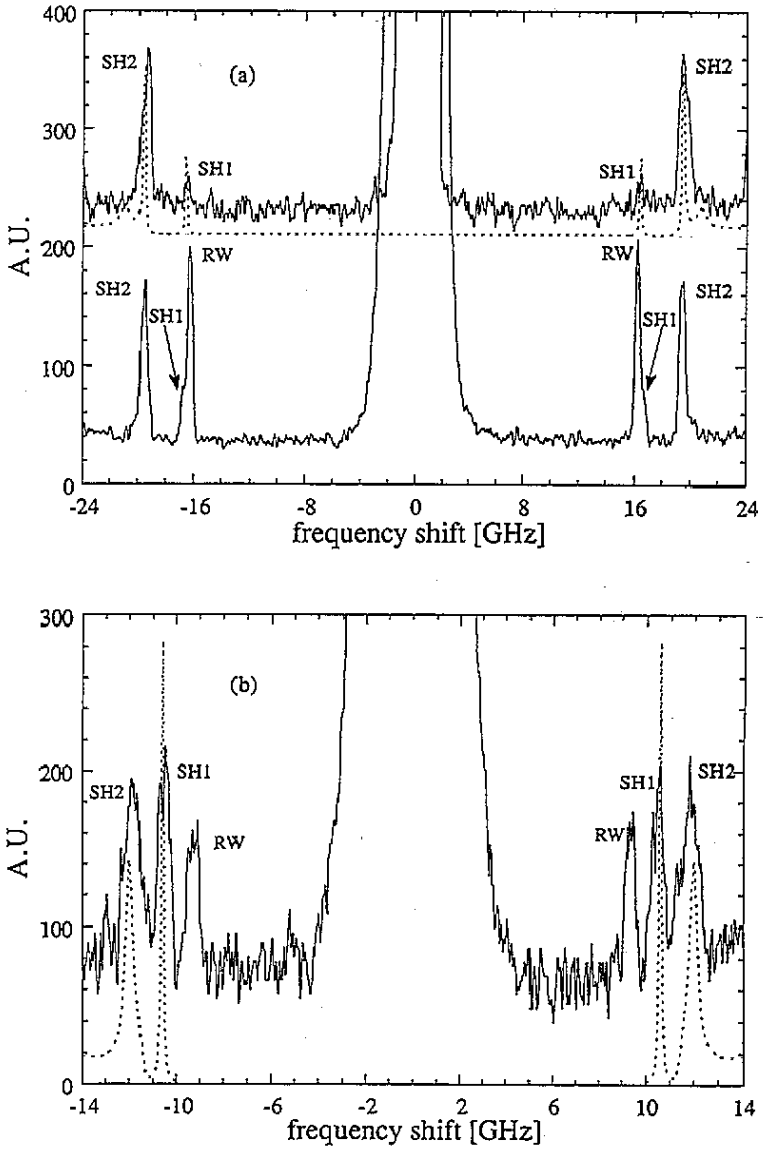

Figure 1. Measured Brillouin spectra along ⟨100⟩ (full line) compared with the calculated integral $S_{yy}(\omega, Q_{\|})$ of the LPPDS (see equation (6)) (dashed line). (*a*) Lower trace, Brillouin spectrum taken at $\theta = 60°$ with no polarization analysis of the scattered field; upper trace, p–s spectrum at $\theta = 60°$. (*b*) Brillouin spectrum taken at $\theta = 30°$ with no polarization analysis of the scattered field.

agreement with the calculated curves and can be explained by the analysis of plots of the LPPDS as a function of depth and frequency computed at the same angles of incidence. These are presented respectively in figures 2(*a*) and (*b*). The plot of $S_{yy}(\omega, Q_{\|})$ at 30° shows a broader peak at SH2, which is also in agreement with experimental results. The larger extension of mode SH1 in the top Si layer when $\theta = 30°$ suggests a stronger contribution to the Brillouin spectrum from this mode since there the elasto-optic coupling is higher.

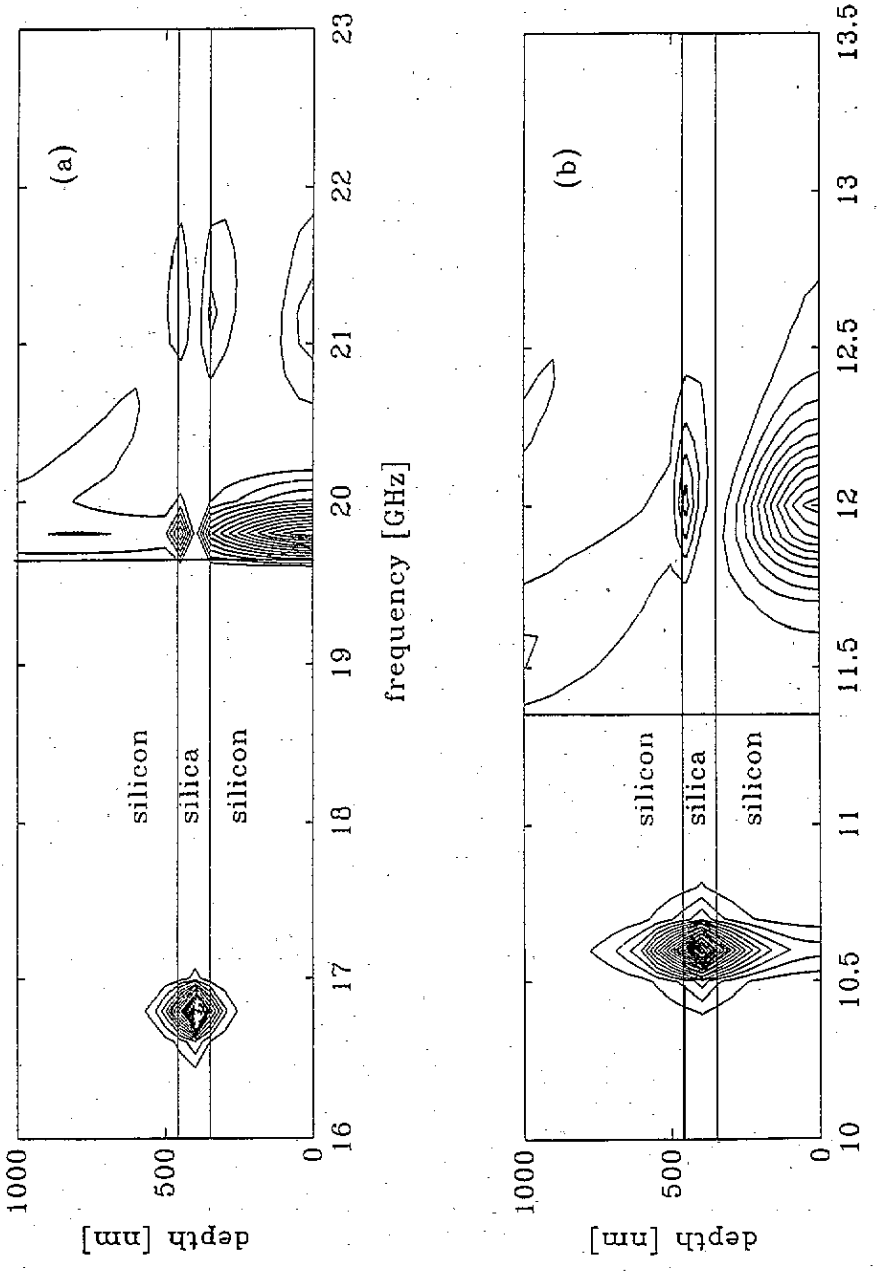

Figure 2. Contour plots of the LPFDS as a function of depth and frequency calculated at 60° (*a*) and 30° (*b*); propagation along ⟨100⟩. In the contour plots the geometry of the sample and the transverse threshold for silicon are evidenced. The first 500 eigenvalues and eigenfunctions of equation (2) were found using the NAG [13] routine D02KEF based on a Prufer transformation and a shooting method. A total slab thickness of 46 000 nm was taken. In equation (4) ϵ was taken to be equal to $2\pi 44$ Mrad s^{-1}.

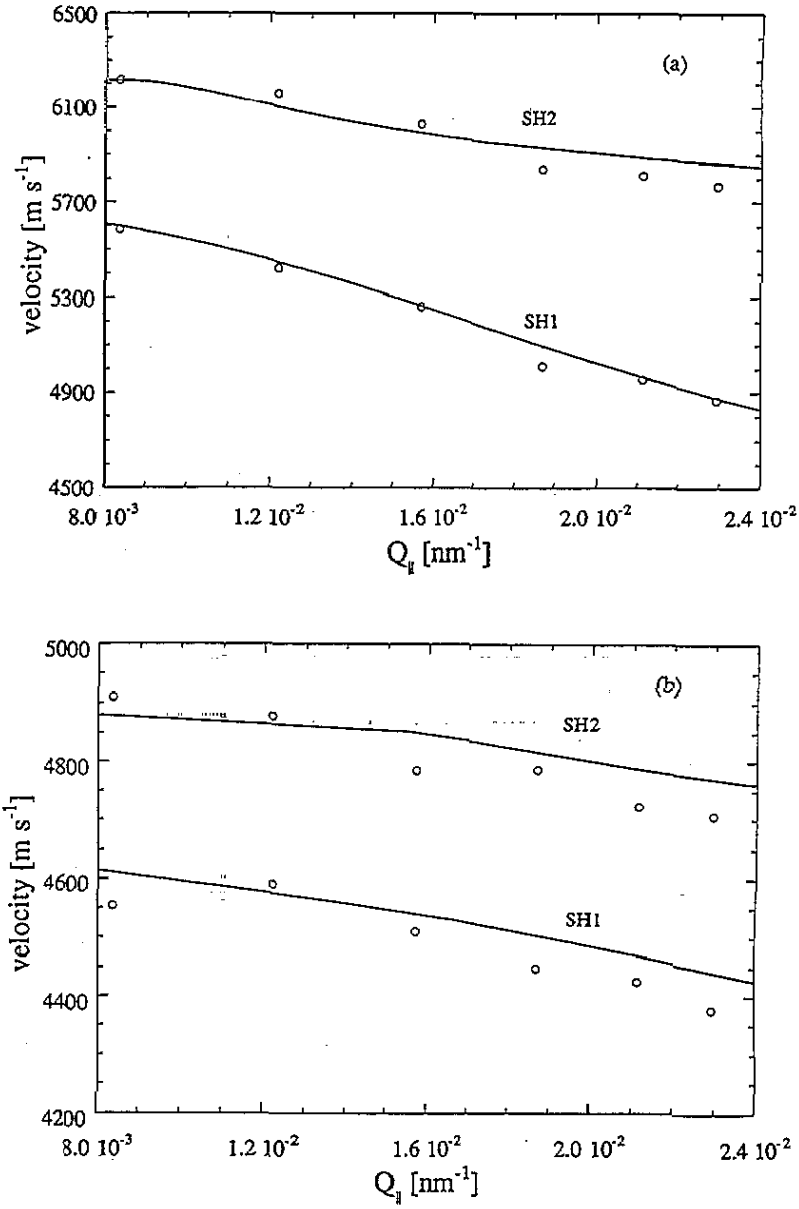

Figure 3. Experimental phase velocity (circles) of modes SH1 and SH2 compared with the theoretical dispersion relations calculated by the $S_{yy}(\omega, Q_{||})$ peak positions; (*a*) (100); (*b*) (110).

This argument can also be applied to explain the high visibility of peak SH2, whose surface character is evident, since the corresponding packet of acoustic waves is strongly localized in the top Si layer. In general we can say that the found high visibility of SH phonons found is a peculiar feature of the geometry and the elasto-optic properties of our samples. This allows for a very significant presence of SH modes in the subsurface Si region where the elasto-optic coupling is quite large and the exciting electric field intense.

From the peak positions in the Brillouin spectra at different incident angles we

determined the dispersion relation for the experimental phase velocity of SH modes SH1 and SH2 along ⟨100⟩ and ⟨110⟩ (figure 3). The continuous curves were calculated by taking the peak positions in $S_{yy}(\omega, Q_{\|})$ evaluated at different angles of incidence. The agreement with the experimental points is fairly good and both curves show a decrease of phase velocity with the parallel wavevector. For the discrete peak SH1 this is due to a larger confinement of the acoustic mode in the slow SiO_2 layer at higher values of parallel wavevector as observable in figure 2.

In conclusion we have given experimental evidence and theoretical explanation of Brillouin scattering from SH surface acoustic phonons in both the discrete and continuum parts of the spectrum in a structure composed of an SiO_2 layer buried in an Si buffer. The discrete spectrum is represented by an SH mode confined in the buried layer while the continuum part shows a main quasi-resonance in the spectrum, which is detected as a peak in Brillouin spectra. The intensity of peaks in the Brillouin spectra has been qualitatively described in terms of the layer projected phonon density of states.

We gratefully acknowledge Dr L Meda and Dr G F Cerofolini of Istituto Donegani (Novara, Italy) for supply of the samples and Mr S Bertoni, of the same Institute, for electron microscopy. Many thanks are due to Professor F Nizzoli for several discussions and encouragement. A particular aknowledgment is due to Dr J R Sandercock for his invaluable technical advise. The presented activity was funded by Progetto Finalizzato *Materiali Speciali per Tecnologie Avanzate* of CNR.

References

[1] Marvin A M, Bortolani V, and Nizzoli F 1980 *J. Phys. C: Solid State Phys.* **13** 299
[2] Bortolani V, Marvin A M, Nizzoli F and Santoro G 1983 *J. Phys. C: Solid State Phys.* **16** 1757
[3] Sandercock J R 1982 *Light Scattering in Solids III (Topics in Applied Physics 51)* ed M Cardona and G Güntherodt (Berlin: Springer) p 173
[4] Loudon R and Sandercock J R 1980 *J. Phys. C: Solid State Phys.* **13** 2609
[5] Bortolani V, Nizzoli F, Santoro G, Marvin A M and Sandercock J R 1979 *Phys. Rev. Lett.* **43** 224
[6] Bortolani V, Nizzoli F, Santoro G and Sandercock J R 1982 *Phys. Rev.* B **25** 3442
[7] Karanikas J M, Sooryakumar R and Phillips J M 1989 *Phys. Rev.* B **39** 1388
[8] Albuquerque E L, Loudon R and Tilley D R 1980 *J. Phys. C: Solid State Phys.* **13** 1775
[9] Bell J A, Zanoni R, Seaton C T, Stegeman G I, Bennett W R and Falco C M 1988 *Appl. Phys. Lett.* **52** 610
[10] Courant R and Hilbert D 1953 *Methods of Mathematical Physics* vol I (New York: Interscience) p 324
[11] Landolt H and Börnstein R 1987 *Numerical Data and Functional Relationships in Science and Technology III* ed O Madelung (Berlin: Springer)
[12] Kaye G W and Laby T H 1986 *Tables of Physical and Chemical Constants* (London: Longman)
[13] NAG 1983 *Fortran Library Manual* Mark 10, vol 2 (Numerical Algorithms Group)
[14] Marvin A, Bortolani V, Nizzoli F and Santoro G 1980 *J. Phys. C: Solid State Phys.* **13** 1607
[15] Primak W and Post D 1959 *J. Appl. Phys.* **30** 779